Review

Not peer-reviewed version

Lubrication Challenges in Deep-Sea Gear Transmissions: A Review of High-Pressure and Low-Temperature Effects

Weiqiang Zou , Xigui Wang * , Yongmei Wang * , Jiafu Ruan

Posted Date: 9 February 2026

doi: 10.20944/preprints202602.0594.v1

Keywords: gear transmission system; deep-sea environment; multi-physics coupling modeling; meshing interface texturing; elasto-hydrodynamic lubrication

 doi:10.20944/preprints202602.0594.v1

Review

Lubrication Challenges in Deep-Sea Gear Transmissions: A Review of High-Pressure and Low-Temperature Effects

Weiqiang Zou [1], Xigui Wang [1,*], Yongmei Wang [2,*] and Jiafu Ruan [1]

[1] School of Mechatronics and Automation, Huaqiao University, No. 668 Jimei Avenue, Jimei District, Xiamen 361021, China

[2] School of Motorcar Engineering, Heilongjiang Institute of Technology, No. 999, Hongqidajie Road, Daowai District, Harbin 150036, China

* Correspondence: wxg1972@hqu.edu.cn or wyr20091207@126.com (X.W.); wyr20091207@163.com (Y.W.); Tel.: +86-13384503780 (X.W.); +86-15045632699 (Y.W.)

Abstract

The extremely high pressure and low temperature inherent to deep-sea environments pose significant challenges for the lubrication performance of gear transmission systems. The synergistic effects of high pressure and low temperature not only cause an exponential increase in lubricant viscosity, leading to reduced fluidity, startup difficulties, and lubrication starvation, but also allow seawater intrusion, which may induce lubricant emulsification, additive failure, and tooth surface corrosion, further exacerbating the risk of lubrication failure. This article reviews recent research progress in gear lubrication under deep-sea high-pressure and low-temperature conditions, with a specific focus on Elasto-Hydrodynamic Lubrication (EHL) theory and gear interface texturing. By thoroughly analyzing deep-sea environmental characteristics and their influence on lubricant properties, this article explores the applicability of Thermal Elasto-Hydrodynamic Lubrication (TEHL) theory in extreme environments. The discussion covers advancements in numerical simulations as well as key challenges. Additionally, the paper elaborates on the anti-friction and wear-resistance mechanisms of interface texturing, emphasizing its ability to improve gear lubrication states and boost tribological performance. Consequently, this study summarizes the limitations of existing research. It proposes future development directions, including multiphysics coupling modeling, synergistic texture and coating design, experimental validation, and engineering applications. Ultimately, this review aims to provide theoretical support and technical references for the reliable design and long-term stable operation of gear transmission systems in deep-sea equipment.

Keywords: gear transmission system; deep-sea environment; multi-physics coupling modeling; meshing interface texturing; elasto-hydrodynamic lubrication

1. Introduction

The ocean harbors abundant biological, mineral, and energy resources, representing a strategic frontier for sustainable development and a vital space for future human progress [1]. The exploration and utilization of these distant and deep-sea resources rely on advanced equipment such as submersibles, seabed drilling systems, underwater robots, and tidal energy generators [2–4]. Within these sophisticated systems, gear transmissions play a pivotal role in power transmission and motion conversion; their performance directly dictates the operational capability, precision, and reliability of the entire equipment [5–7]. Unlike terrestrial environments, this equipment typically operates hundreds or thousands of meters underwater, subject to extreme hydrostatic pressure, low temperatures, and a highly corrosive saline environment [8,9]. This coupled high-pressure and low-

 doi:10.20944/preprints202602.0594.v1

temperature setting poses unprecedented challenges to materials, structures, and lubrication. As equipment descends into deeper waters, the pressure differential across the gearbox increases dramatically. If uncontrolled, the immense external pressure can deform the housing structure and compromise sealing systems, leading to seawater intrusion [10]. To mitigate the immense pressure differentials in deep-sea environments, systems typically employ pressure-balancing devices to maintain pressure equilibrium within the gearbox. Figure 1 shows standard pressure compensation units, including the elastic bladder (see Figure 1a) and moving piston (see Figure 1b) types, along with the shuttle pin design featuring dual-bladder PBOF technology from Siemens DigiTRON (see Figure 1c) [11,12]. Although this strategy protects the housing from deformation, it exposes the internal components to high ambient pressure, altering the lubricant's physicochemical properties. Specifically, high pressure significantly increases oil viscosity and flow resistance, potentially causing additive instability or changes in solubility. Consequently, this inevitably impairs lubricant film formation and load-bearing capacity, accelerates wear, and reduces the equipment's operational lifespan.

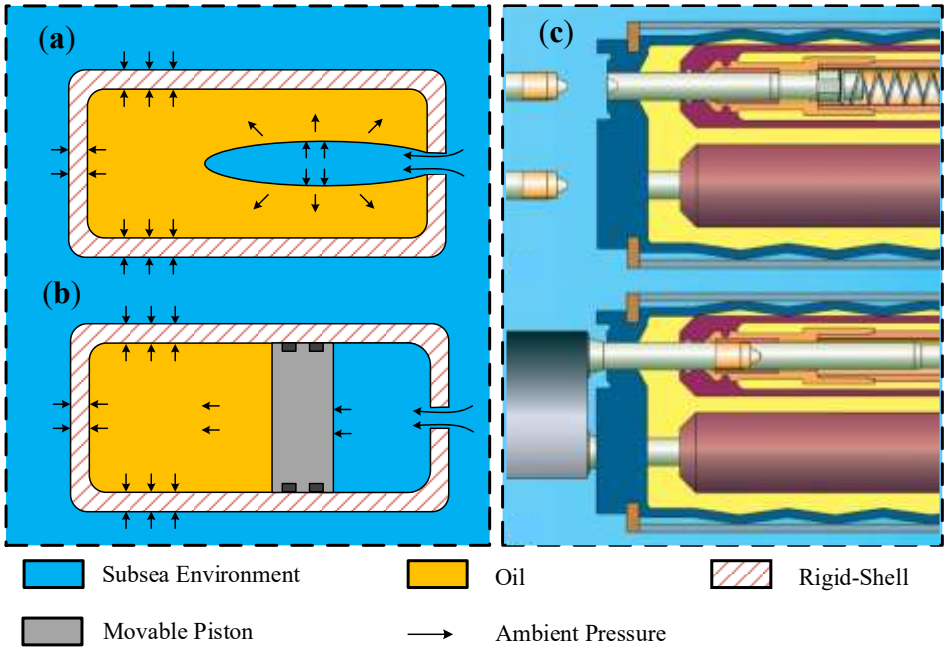

Figure 1. Schematic illustration of the mechanism of pressure-balanced units: (a) resilience-bladder type, (b) movable-piston type, (c) the shuttle pin design with dual-bladder PBOF technology of Siemens DigiTRON.

Under high-pressure conditions, the viscosity of lubricating oil increases exponentially, leading to a sharp decline in fluidity that can induce a semi-solid state [13]. This not only significantly increases churning power loss within the gearbox but also impedes timely backflow and oil replenishment, resulting in film rupture and exacerbated tooth surface wear [14,15]. The high-pressure environment places stringent demands on sealing systems; seal failure can lead to high-pressure seawater intrusion, contaminating the lubricant, corroding gear surfaces, and potentially triggering complex failures such as fretting corrosion [16,17]. Furthermore, temperatures in most deep-sea regions remain between 2 and 4 °C year-round. These low temperatures further increase viscosity and reduce fluidity [18]. Under the combined effects of high pressure and low temperature, the dramatic rise in viscosity leads to higher starting torque and reduced pumping performance, making it challenging to supply lubricant to the meshing zone promptly and thereby causing lubrication starvation [19]. Moreover, high pressure and low temperature alter critical thermophysical parameters, such as density and thermal conductivity, compromising the accuracy of film thickness and temperature field calculations in Thermal Elasto-Hydrodynamic Lubrication (TEHL) analysis. In extreme cases, such as during cold starts, the drastic viscosity increase may

 doi:10.20944/preprints202602.0594.v1

prevent startup altogether [20,21]. As the core theory for studying lubrication in high-load, non-conformal contacts, TEHL comprehensively accounts for hydrodynamic effects, elastic deformation, and the lubricant's pressure-viscosity and temperature-viscosity characteristics, alongside thermal effects. It accurately describes key parameters in the meshing zone, such as film pressure, thickness, temperature field, and friction [22–24]. By establishing numerical models that reflect the coupled effects of high pressure and low temperature, applying TEHL theory to deep-sea gear systems enables the quantitative analysis and prediction of lubrication characteristics under extreme operating conditions [25]. However, relying solely on passive selection of superior lubricants and base materials is often insufficient to address such harsh conditions fully. Interface texturing technology, an active tribological control strategy, has garnered significant attention in recent years [26]. This technique involves creating micro-scale pits or grooves with specific geometries and spatial arrangements on friction pair surfaces to improve lubrication and suppress friction and wear. Through mechanisms such as acting as oil reservoirs, generating secondary hydrodynamic effects, and trapping wear debris, interface texturing offers a promising solution for addressing the lubrication challenges faced by deep-sea gears under high loads and low speeds.

While traditional research on gear lubrication has achieved substantial success under conventional conditions, it remains inadequate for addressing extreme marine environments characterized by high pressure and low temperatures. Adequate lubrication is essential for reducing friction and wear, lowering energy consumption, and extending equipment service life; however, traditional lubrication theories and methods often prove insufficient in deep-sea, high-pressure, and low-temperature environments. Consequently, this article reviews and evaluates the progress of two core research areas, Elasto-Hydrodynamic Lubrication (EHL) theory and interface texturing technology, within the context of marine gear transmission systems. Through an in-depth analysis of the mechanisms by which extreme environments affect lubrication performance, future research prospects are outlined. This study aims to provide theoretical support for the reliable design and operation of marine transmission systems, offering valuable insights and engineering guidance for enhancing the performance and reliability of deep-sea equipment.

2. Lubricant Interactions in Deep-Sea Extremes: A Review of Environmental Characteristics and System Responses

2.1. Multi-Scale Parametric Characteristics of Deep-Sea Environments: Pressure and Temperature

In contrast to terrestrial operating environments, marine gear systems operate in a significantly more severe service environment, compounded by high pressure and low temperatures. As operational depths reach several thousand meters, systems must adapt to these extreme conditions. The deep sea, commonly defined as depths exceeding 200 m or, more strictly, below 1000 m, constitutes over 95% of the Earth's habitable biosphere and represents the planet's most extensive and least understood ecosystem [27]. Seawater temperature drops noticeably with depth, stabilizing only after passing through the thermocline into the abyssal and hadal zones [28]. Beginning at approximately 200 m depth, seasonal and interannual temperature fluctuations essentially vanish, creating a highly stable cold environment throughout the global deep ocean where water temperatures are consistently maintained between 0 and 4 °C [29,30]. Concurrently, hydrostatic pressure increases sharply, rising linearly at a gradient of about 0.1 MPa per 10 m, exceeding 110 MPa at the extreme depths of the Mariana Trench [31,32]. Furthermore, light intensity decays exponentially with depth, with 99% of incident light dissipated by 150 m, rendering the environment below 250 m virtually devoid of light [33,34]. Chemically, seawater acts as a strong electrolyte, rich in chloride ions and dissolved oxygen, and constitutes a naturally corrosive environment [35]. In this aqueous setting, metals form microscopic anodic and cathodic regions where anodic metal dissolution and cathodic oxygen reduction reactions occur. Notably, the high concentration of chloride ions is highly aggressive and can break down the passivation film on metal surfaces, thereby initiating and accelerating localized corrosion [36]. Prolonged exposure to this high-salinity, high-

 doi:10.20944/preprints202602.0594.v1

humidity environment poses severe electrochemical corrosion challenges for metallic materials. This not only significantly compromises the load-bearing capacity of materials but also contributes to the premature failure of gear transmission systems.

2.2. Thermodynamic and Rheological Responses of Lubricants to Deep-Sea Pressure-Temperature

At low temperatures, the thermal motion of molecules is suppressed, allowing intermolecular forces to dominate and molecular structures to become more ordered. This phenomenon increases flow resistance and elevates viscosity. As temperature rises, however, intermolecular separation expands and cohesive forces decline; the resulting enhancement in molecular thermal motion reduces flow resistance, manifesting macroscopically as a substantial decrease in viscosity [37,38]. On the other hand, increasing pressure compresses lubricant molecules, reducing the average intermolecular distance and free volume. These intensified interactions lead to a marked increase in flow resistance and an exponential increase in viscosity [39]. Consequently, within the framework of EHL theory, lubricant viscosity is commonly defined as a function of both pressure and temperature.

Since the 19th century, researchers have developed various empirical and semi-empirical models to characterize the dependence of lubricant viscosity on temperature and pressure. These models generally fall into three categories: viscosity-temperature equations, viscosity-pressure equations, and coupled viscosity-temperature-pressure equations that account for both factors simultaneously. Among viscosity-temperature models, the Reynolds equation is suitable for narrow temperature ranges, whereas the Andrade equation, despite its simple form, has limited predictive capability over broad temperature spans [40–42]. The Slotte equation more accurately describes viscosity changes across wide temperature variations, although its parameters are fluid-specific [43]. The Vogel-Fulcher-Tammann (VTF) equation, grounded in free volume theory, is particularly effective for describing viscosity behavior near the glass transition [44]. The Walther equation, recommended as an ASTM standard, serves as the basis for generating viscosity-temperature charts. Regarding viscosity-pressure relationships, the Barus equation is simple but applicable only to low pressures; the Roelands equation offers superior accuracy over a wider pressure range, while the Cameron equation can be viewed as a modification of the Barus model suited for high-pressure conditions [45,46]. In practical operating scenarios, such as EHL, temperature and pressure often fluctuate drastically and simultaneously, necessitating the use of coupled models. For instance, the Barus-Reynolds combination is straightforward but inherits the high-pressure inaccuracies of the Barus model. Since its introduction in 1966, the Roelands equation has gained widespread recognition for its accuracy and universality across diverse conditions. To provide a unified description of viscosity behavior from the liquid to the glassy state, researchers have also developed comprehensive models such as the WLF-Yasutomi model. By integrating the WLF equation with the Tait equation of state, this model effectively predicts viscosity variations across a range of pressures and temperatures within a single framework. Continuously refined through experimental fitting, it has become one of the most representative models in current use [47–49].

Table 1. Lubricating Oil Relations.

Type	Model	Formula	Equation number
Viscosity–temperature correlation	Reynolds	$\eta = \eta_0 e^{-\beta(T-T_0)}$	(1)
	Andrade-Erying	$\eta = \eta_0 e^{\frac{\alpha}{T}}$	(2)
	Slotte	$\eta = \frac{s}{(\alpha + T)^m}$	(3)
	Vogel	$\eta = \eta_0 e^{b/(T+\theta)}$	(4)
	Walther	$(v+a) = bd^{1/T^c}$	(5)

 doi:10.20944/preprints202602.0594.v1

Viscosity–pressure correlation	Barus	$\eta = \eta_0 e^{\alpha p}$	(6)
	Roelands	$\eta = \eta_0 e^{\left\{(\ln \eta_0 + 9.67)\left[-1+(1+p_0 p)^z\right]\right\}}$	(7)
	Cameron	$\eta = \eta_0 (1+cp)^{16}$	(8)
Viscosity–temperature–pressure correlation	Barus and Reynolds	$\eta = \eta_0 e^{\left[\alpha p - \beta (T - T_0)\right]}$	(9)
	Roelands	$\eta = \eta_0 e^{\left\{(\ln \eta_0 + 9.67)\left[\left(1+5.1\times10^{-9} p\right)^{0.69} \times \left(\frac{T-138}{T_0-138}\right)^{-1.1} - 1\right]\right\}}$	(10)
	WLF-Yasutom	$\eta = \eta_g e^{\left(\log(10)\frac{-C_1 (T - T_g(p)) F(p)}{C_2 + (T - T_g(p)) F(p)}\right)}$	(11)

Under high-pressure operating conditions typical of deep-sea environments, hydrostatic pressures reaching tens of megapascals are sufficient to induce a significant increase in the base viscosity of lubricating oil. In Hertzian contact zones, pressures can surge to the gigapascal (GPa) range, increasing viscosity by several orders of magnitude. Accurately modeling such drastic variations is critical for TEHL analysis. Concurrently, the low-temperature environment of the deep sea can elevate lubricant viscosity by one to two orders of magnitude compared to ambient conditions. While increased viscosity theoretically facilitates the formation of thicker oil films, the adverse effects of severely reduced fluidity are more pronounced and often constitute the primary cause of lubrication failure. The synergistic effect of high pressure and low temperature drives the lubricating oil into an extreme high-viscosity state, where its behavior approximates that of an amorphous solid, exhibiting extremely high internal friction and shear stress. This state further acts as a significant source of churning losses and temperature escalation within the contact zone. Consequently, precise characterization and simulation of the viscosity-pressure-temperature relationship under these coupled high-pressure and low-temperature conditions are crucial prerequisites for reliable lubrication analysis and design. However, the experimental data under such extreme conditions remain extremely scarce.

2.3. Lubricant Density: A Foundation for Thermophysical Property Estimation and Performance Prediction

Beyond viscosity, thermophysical properties such as density, thermal conductivity, and specific heat capacity are pivotal in TEHL analysis because they directly affect the solution of the mass conservation and energy equations. These properties depend significantly on temperature and pressure, a sensitivity that intensifies under extreme operating conditions. Density, a key parameter, substantially affects the fluid mass flowing through the contact zone and the oil film thickness. Research indicates that density typically decreases with rising temperature and increases with rising pressure [50]. Owing to its concise form and ease of application, the Dowson-Higginson equation is widely used in engineering calculations:

$$\rho(p,T) = \rho_R \left\{ \frac{5.9\times10^8 + 1.34p}{5.9\times10^8 + p} - \beta_{DH}(T - T_R) \right\} \quad (12)$$

where, ρ_R is the reference density, T_R is the reference temperature, and β_{DH} is the density-temperature coefficient.

To further enhance prediction accuracy across a wide range of pressures and temperatures, the Tait [51] equation of state is more precise than the Dowson-Higginson equation:

$$\rho(p,T) = \frac{\rho_R}{\{1+\alpha_\upsilon (T - T_R)\}\left\{1 - \frac{1}{1+K_0^{'}} \ln\left[1 + \frac{(1+K_0^{'})p}{K_\infty e^{-\beta_K T}}\right]\right\}} \quad (13)$$

 doi:10.20944/preprints202602.0594.v1

where, α_υ is the coefficient of volumetric thermal expansion, $K_0^{'}$ is the variation of the isothermal bulk modulus at absolute zero temperature, K_∞ is the isothermal bulk modulus at absolute zero temperature, and β_K is the temperature coefficient of the isothermal bulk modulus.

Thermal conductivity and specific heat capacity define a lubricant's capacity for heat transfer and thermal storage, respectively. Together, these parameters govern the temperature profile within the TEHL contact zone. While both properties exhibit pressure and temperature dependence, the sensitivity of their variation is generally less pronounced than that of viscosity and density. Typically, thermal conductivity increases slightly with increasing pressure and temperature, whereas specific heat capacity is primarily temperature-dependent, with pressure playing a negligible role. In low-temperature environments, reduced thermal conductivity can impede the dissipation of shear-induced heat, leading to additional localized temperature spikes. This phenomenon may initiate a complex coupled feedback loop characterized by rising temperatures, decreased viscosity, and consequent variations in shear heat generation.

2.4. Seawater Ingress-Induced Multiscale Degradation of Deep-Sea Gearbox Lubricant: Damage Mechanisms, Performance Prediction, and Intrusion-Resistant Technology

Sealing systems represent a critical weak point in deep-sea equipment. Subjected to sustained high differential pressures, they face a significant risk of failure. If seawater infiltrates the gearbox, it drastically reduces the lubricant's apparent viscosity, impairing film formation and shifting from hydrodynamic to mixed or boundary lubrication, thereby accelerating wear on friction pairs [52]. As illustrated in Figure 2, the phase behavior of oil-water mixtures is complex. At water concentrations below the saturation limit, water dissolves into the oil, creating a homogeneous solution with a viscosity lower than that of the pure base oil [53]. Beyond this limit, an unstable two-phase system develops, characterized by water dispersed as fine droplets. While initial water addition slightly increases viscosity due to heightened interfacial tension [54], exceeding a critical concentration triggers an emulsion inversion from water-in-oil (W/O) to oil-in-water (O/W). This results in a precipitous decline in viscosity and a consequent loss of the lubricating film's load-bearing capacity. Moreover, electrolytes and chloride ions inherent in seawater can disrupt the oil-water interfacial tension and compromise the metal's passive film. The synergistic effect of mechanical wear and electrochemical corrosion significantly accelerates material degradation, fostering a vicious cycle of corrosion-promoting-wear and wear-promoting-corrosion [55–57].

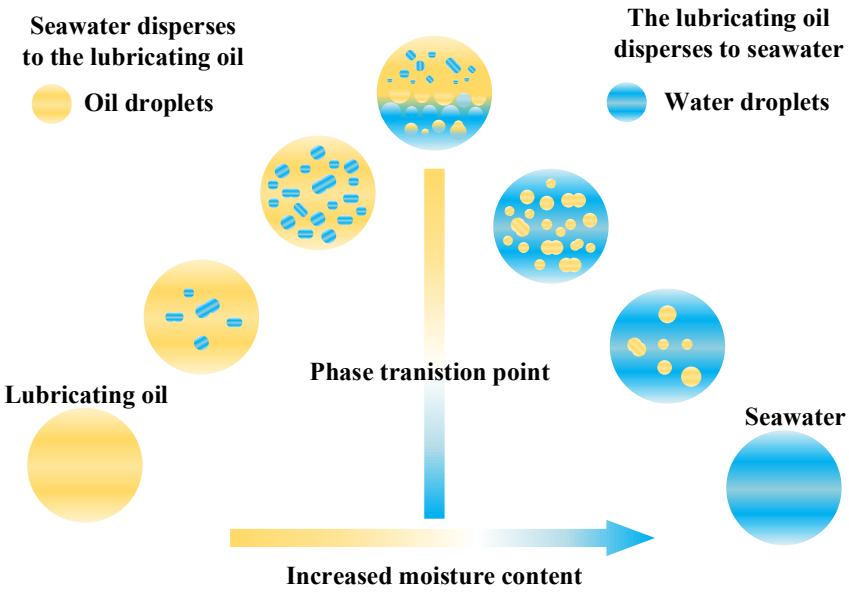

 doi:10.20944/preprints202602.0594.v1

Figure 2. Schematic diagram of oil-water two-phase state.

Moreover, seawater can induce hydrolysis or chemical reactions with extreme pressure and anti-wear additives, thereby neutralizing their efficacy and inhibiting protective film formation under boundary lubrication regimes [58]. Seawater also disrupts the suspension stability of additives and accelerates the hydrolytic degradation of ester-based environmentally friendly lubricants. The resulting production of acidic species and sludge intensifies the corrosion of metal components [59,60]. This deterioration not only diminishes lubrication performance but also risks clogging filters and oil passages, potentially leading to oil starvation and threatening the integrity of the lubrication system.

3. EHL Theory in Ultra-Deep Marine Conditions: Adaptive Mechanisms, Key Challenges, and Frontiers

3.1. Multi-Physics Coupling Effects on Lubrication Regime Transitions in Deep-Sea Gear Transmission Meshing Interfaces

The Stribeck curve delineates three distinct lubrication regimes for mechanical contacts: full-film, mixed, and boundary lubrication. Full-film lubrication principally comprises hydrodynamic lubrication and EHL. In the context of heavily loaded gear pairs, the operating regime typically spans the spectrum from EHL to mixed lubrication. Figure 3 schematically delineates the characteristic features of these regimes and their transition dynamics. Under hydrodynamic and elastohydrodynamic conditions, contacting surfaces are entirely separated by a lubricant film of adequate thickness. Friction primarily arises from the internal shearing of lubricant molecules. In this state, the coefficient of friction is markedly low, wear is negligible, and the system operates under ideal lubrication conditions. Boundary lubrication stands in stark contrast; here, the lubricant film is extremely thin or non-existent, and the load is borne almost entirely by direct asperity contact. Consequently, this regime is characterized by high friction coefficients and severe wear. Mixed lubrication represents the intermediate state, where the load is distributed between the fluid film and asperity contacts, resulting in complex tribological behavior. Under the high-pressure, low-temperature conditions unique to deep-sea environments, lubricant viscosity increases exponentially, profoundly influencing the lubrication regime. Within the full-film regime, increased viscosity promotes the formation of a thicker lubricant film, thereby bolstering surface protection. In the mixed regime, higher viscosity mitigates direct asperity contact, reducing wear. Conversely, in the boundary regime, protection relies primarily on surface-adsorbed chemical films. Nevertheless, the extreme viscosity elevation in such severe environments complicates the lubricant's rheological behavior, posing a potential threat to the transmission system's operational reliability.

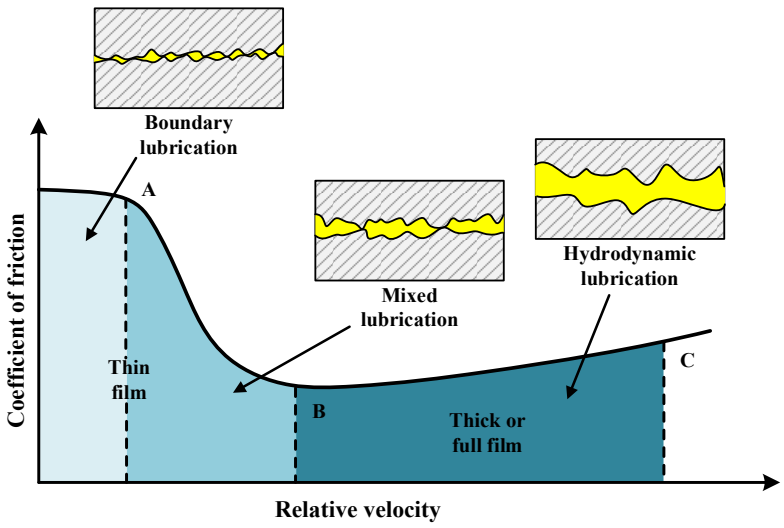

 doi:10.20944/preprints202602.0594.v1

Figure 3. Transition of Lubrication Regimes.

High hydrostatic pressure in the deep sea can induce the glass transition of lubricants, leading to a sharp increase in the molecular relaxation time and a shift in dynamic behavior from liquid-like to solid-like, thereby forming a macroscopic friction plateau [61,62]. At low temperatures, lubricants exhibit diverse phase behaviors: mineral oils may exhibit shear-thinning and yield stress driven by paraffin crystallization, whereas synthetic oils may undergo a glass transition, leading to a nonlinear increase in viscosity [63]. These transitions significantly compromise the spreading capability of the oil film, expediting the shift from EHL to mixed or even boundary lubrication regimes [64,65]. Models of rough surface contact further validate that increased surface roughness or reduced load shortens the window for the onset of mixed lubrication; notably, wear frequently initiates at the point of minimum film thickness along the contact zone periphery [66]. In light of the limitations of conventional lubricants in marine settings, solid lubricants suitable for extreme temperatures have emerged as a critical solution. This category encompasses layered materials, soft metals, MAX phases, and stable fluorides and oxides. Self-lubricating composites manufactured via powder metallurgy or thermal spraying techniques provide adequate lubrication across a broad temperature range [67]. Simultaneously, environmentally friendly gel lubricants retain advantageous rheological properties at low temperatures, showing promise for use in polar and deep-sea applications [68].

3.2. TEHL Theory for Gears Operating Under High-Pressure and Low-Temperature Conditions

The theory of TEHL for gears comprehensively accounts for the coupling effects of elastic deformation, thermal phenomena, and hydrodynamic lubrication during meshing. This approach enables a more realistic prediction of oil film thickness, pressure distribution, and temperature within the contact zone, thereby facilitating the assessment of performance indicators such as friction, wear, and fatigue [69]. Building upon isothermal EHL theory, TEHL introduces the energy equation to account for frictional heating. The formulation centers on solving a system of highly nonlinear partial differential equations that characterize the physical state of the lubricated contact. A comprehensive TEHL numerical model generally comprises the Reynolds equation, the film thickness equation, the load balance equation, the energy equation, and rheology equations governing the viscosity-pressure-temperature relationship. Numerical techniques are utilized to determine the pressure, thickness, and temperature distributions of the lubricant film. Figure 4 presents a schematic diagram of the pressure distribution and the variation in film thickness.

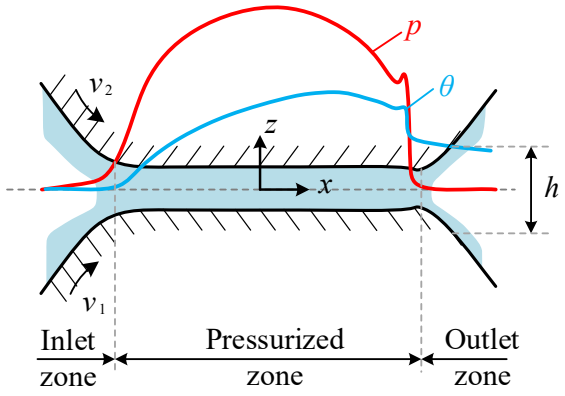

Figure 4. Schematic of pressure distribution and film thickness variation in the lubricating film.

The lubrication regime of gear meshing falls within the EHL domain, requiring the concurrent consideration of elastic deformation in the contacting bodies and variations in lubricant viscosity. During actual operation, gear surfaces endure extreme contact pressures, combined rolling and sliding motions, and transient thermal effects, creating a complex TEHL scenario. TEHL theory

 doi:10.20944/preprints202602.0594.v1

comprehensively accounts for the coupling among thermal effects, elastic deformation, and hydrodynamics, providing a realistic representation of the lubrication state. Under high-pressure and high-speed transmission, transient temperature elevations in the contact zone further intensify this complexity. Liu et al. [70] elucidated the mechanism by which unbalanced radial forces in high-pressure internal gear pumps induce gear deformation, thereby shifting the dominant frequency of pressure pulsation and integrating dynamic loads with a mixed EHL model. Xiao et al. [71] clarified the evolutionary patterns of gear lubrication parameters under high loads and speeds. Nevertheless, extreme operating conditions present severe challenges to lubrication stability. Duan et al. [72] found that, upon reaching critical load and speed values, the friction coefficient increases sharply when oil temperature exceeds the flash point, precipitating lubrication failure and severe wear. The oil film stiffness model established by Yin et al. [73] demonstrated that thermal-induced temperature rise reduces lubricant viscosity and increases compressive deformation of the oil film, resulting in tangential stiffness significantly higher than that predicted by isothermal assumptions. This phenomenon is particularly pronounced in the tooth root region, where loads are concentrated. Wang et al. [74] developed a finite-element coupling model to investigate mixed lubrication in planetary gear systems under low-speed, heavy-load conditions, accounting for local temperature rises from asperity contact, film rupture, and thermal deformation.

In contrast, low-temperature environments significantly impact lubricant properties and system behavior. Research by Su et al.[75] suggests that low temperatures drastically increase lubricant viscosity and alter its rheology. This results not only in oil film thickening and abnormal fluctuations in the traction coefficient, but also in exacerbated rolling-element slippage. To accurately capture rheological behavior under low-temperature, high-viscosity conditions, Gao et al. proposed a modified Herschel–Bulkley model, which exhibits superior accuracy in fitting experimental data and calculating engineering traction coefficients compared to traditional H-B and T-J models. Moreover, a mechanical-thermal coupling model by Liu et al. [76] revealed that increased grease viscosity at low temperatures in high-speed train bearings leads to film thickening and aggravated slippage, identifying these factors as intrinsic causes of early failures in cold-region rail bearings. Lastly, employing a viscous-hyperelastic mixed lubrication model, Wang et al. [77] demonstrated that in deep-sea environments defined by high pressure, low temperatures, and corrosion, their model offers significantly better prediction accuracy for water film stiffness than traditional linear models, offering critical theoretical support for the design of water-lubricated gear transmissions.

3.3. Applicability and Challenges of EHL in Deep-Sea Environments

Under ultra-high hydrostatic pressure, conventional viscosity-pressure relationships often fail to characterize lubricant behavior accurately. As pressure approaches the glass transition point, the constitutive behavior deviates significantly from standard models [78,79]. Furthermore, high pressure compresses the lubricant substantially, increasing its density. This change directly impacts the accuracy of mass conservation and oil film thickness predictions in TEHL calculations [80]. The deep-sea environment creates a unique “cold-exterior, hot-interior” scenario. While the system is externally cooled by low-temperature seawater, the internal high-speed shearing of gear surfaces generates substantial frictional heat. This severe temperature gradient complicates heat conduction and convection, imposing stricter requirements for calculating oil film temperature fields and flash temperatures [81]. Although strong external cooling helps suppress temperature rise and maintain higher oil film viscosity, it complicates thermal management. Consequently, TEHL modeling requires modified boundary conditions to reflect forced convection with seawater, and the impact of thermal management measures, such as insulation layers or active cooling, on the system’s thermal balance must be accounted for [82,83] Extremely low ambient temperatures cause a sharp increase in lubricant viscosity and reduced fluidity [84]. Although high viscosity theoretically promotes thicker oil film formation, the lubricant may fail to replenish the contact zone in time under low-speed conditions where hydrodynamic effects are weak. This can force gears into a mixed or boundary lubrication regime, significantly increasing the risk of wear [85]. During operation, shear heat in the

 doi:10.20944/preprints202602.0594.v1

meshing zone gradually raises the oil temperature, reducing viscosity and potentially shifting the lubrication state toward full-film EHL [86]. However, the deep-sea, low-temperature environment acts as a continuous cold sink, absorbing system heat and maintaining a thermal equilibrium temperature far below normal operating conditions, thereby further affecting lubricant performance and oil film formation. The combination of high hydrostatic pressure and Hertzian contact pressure leads to extremely high lubricant viscosity within the contact zone. This excessive viscosity increases viscous shear forces, leading to a higher friction coefficient and a significant temperature rise. The resulting temperature rise reduces viscosity, thereby limiting the sustained growth of oil film thickness [87]. Since gear meshing is inherently a transient process with continuously changing contact geometry, load, and speed, extreme physical property variations in the deep sea can cause severe fluctuations in lubrication state within a single meshing cycle, making prediction and control significantly more difficult [88,89]

The extreme viscosity resulting from high pressure significantly increases the computational difficulty of solving the TEHL governing equations, often leading to convergence and stability issues in numerical simulations. In these conditions, lubricants may exhibit solid-like shear behavior, leading to a drastic increase in friction and challenging the validity of the traditional Reynolds equation, which is predicated on fluid assumptions [90]. Although recent research has focused on material property models for extreme environments, a model that accurately describes lubricant rheology under the simultaneous influence of low temperature, ultra-high pressure, and high shear rates is still lacking [91] Moreover, the interplay between time-varying frictional heat and rough surfaces with multi-scale fractal characteristics adds further complexity to the analysis of TEHL behavior [92].

4. Meshing Interface Texturing Technology and Its Application Prospects in Deep-Sea Gear Lubrication

4.1. Mechanisms of Friction Reduction and Wear Resistance in Micro-Textured Meshing Interfaces

Meshing interface texturing entails the precise design and fabrication of micro- and nanoscale surface features, such as pits or grooves with specific geometries and spatial distributions, on friction pairs. This approach actively tailors the tribological properties of the interface [93,94]. By modifying surface morphology, texturing regulates lubricant flow and optimizes contact stress distribution, thereby enhancing macroscopic tribological performance. Specific benefits include reduced friction coefficients, improved load-carrying capacity, minimized wear, and effective containment of wear debris [95]. Driven by advancements in precision manufacturing, particularly laser processing, the technique has been widely adopted in mechanical seals, bearings, and piston rings. Moreover, it holds considerable promise for mitigating lubrication challenges in heavily loaded, high-speed gear systems [96,97].

The tribological benefits of interface texturing, specifically friction reduction and wear resistance, stem from the synergy of multiple mechanisms: hydrodynamic pressure enhancement, secondary lubrication, debris entrapment, and surface strengthening. Figure 5a depicts the mechanisms of debris entrapment and cavitation generation on textured surfaces. In hydrodynamic or mixed lubrication regimes, micro-textures establish microscopic wedge-shaped gaps that disrupt the parallel flow of the lubricant film, inducing a convergent zone downstream of the structures [98]. Based on the Reynolds equation, this convergent zone generates additional hydrodynamic pressure, increasing the oil film thickness and separating the contact surfaces. By converting solid-solid contact to fluid shear, this mechanism significantly mitigates friction and wear [99,100] (Figure 5b). During boundary lubrication or transient phases, such as start-stop operations, interface textures act as micro-reservoirs [101,102]. Stored lubricant is released to compensate for insufficiencies in the main oil film, creating a secondary lubricating film that delays or avoids dry contact. This capability markedly improves the reliability of gears operating under severe conditions, such as low speed and heavy load [103,104] (Figure 5c). Additionally, interface textures serve to trap and isolate wear debris,

 doi:10.20944/preprints202602.0594.v1

thereby preventing three-body abrasion at the interface [105,106] (Figure 5d). Moreover, high-energy beam machining techniques, such as laser texturing, induce rapid thermal cycling that modifies the microstructure surrounding the textures. This results in fine-grain strengthening and increased dislocation density, forming hardened zones with elevated microhardness that further bolster the material's resistance to plastic deformation and wear [107].

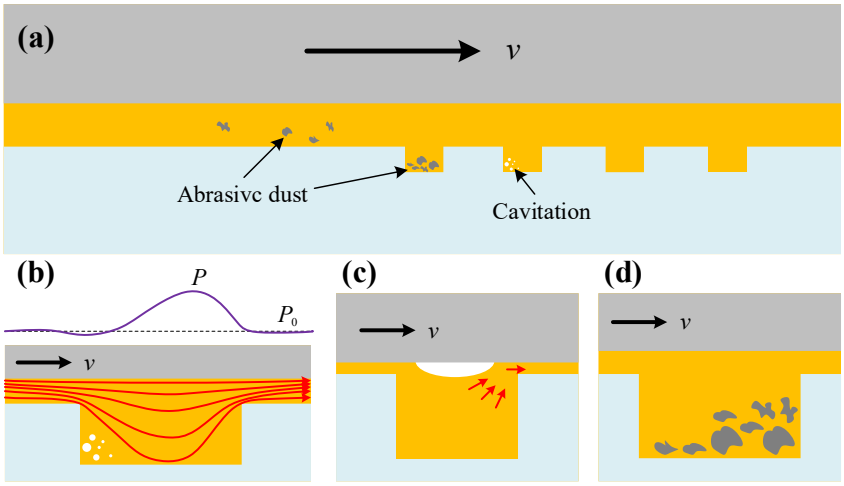

Figure 5. Schematic diagram of the anti-wear mechanisms of interface texturing under different operating conditions.

These interface texturing mechanisms prove particularly effective in marine environments. Under high-pressure conditions, the textures' capacity to store oil compensates for lubricant displacement, thereby maintaining the integrity of the lubricating film. In humid or water-rich environments, the geometric structure helps collect and divert water, thereby alleviating lubricant emulsification. Additionally, during cold starts, the lubricant reservoir within the textures rapidly activates, forming a film that markedly reduces wear during the critical start-up period.

4.2. Micro-Texturing Technologies for Gear Meshing Interfaces: From Lubrication Mechanisms to Anti-Scuffing Load-Bearing Applications

Gear surface texturing is regarded as a pivotal approach for enhancing the tribological performance of gears. Its research scope has progressively evolved from early investigations of simple geometric configurations to the deep integration of biomimetic designs and multi-parameter collaborative optimization. Preliminary explorations primarily focused on analyzing the mechanisms by which basic geometric features, such as circles and grooves, influence gear performance. Tang et al. [108] demonstrated through comparative studies that circular pits effectively reduce the friction coefficient, while Chang et al. [109] via parameter optimization, confirmed that rationally designed groove textures can significantly decrease the surface damage rate and improve anti-adhesion capability, as illustrated in Figure 6a. Inspired by surface morphologies found in nature, biomimetic texturing has emerged as a significant research direction. Lei et al. [110] developed a striped surface inspired by intertidal bivalves, which improved the contact fatigue resistance of gears by more than 20%. Figure 6b displays the curved groove texture designed by Zhang et al. [111] drawing inspiration from the Pecten maximus (great scallop); this design exhibited superior performance in reducing the friction coefficient, wear depth, and operating temperature. Furthermore, the biomimetic hexagonal texture with bidirectional grooves designed by Wang et al. [112] significantly improved thermal management and extended gear service life by enhancing convective heat transfer and lubricant distribution, as shown in Figure 6c.

To further improve performance, the research focus has shifted towards the precise optimization of key texture parameters and their coupling effects within multi-physics fields. Through modeling

 doi:10.20944/preprints202602.0594.v1

and analysis of rhombic micro-textures, Wang et al. [113] found that these textures can reduce the friction coefficient by up to 22.96% and revealed the coupling influence of texture parameters on lubrication and vibration performance. Zhao et al. [114] compared various biomimetic micro-textures and confirmed that the crescent texture, owing to its superior hydrodynamic effect and debris storage capacity, can minimize friction and wear to the greatest extent. Adaptability to operating conditions is also a focal point of research. Gupta et al. [115–117] noted that micro-cylindrical pits are suitable for vibration reduction and debris capture under fully lubricated conditions. In contrast, vertical ellipsoid pits offer superior cooling and vibration suppression in lubrication-starved scenarios, as illustrated in Figure 6d. Furthermore, Tang et al. [118] proposed a manufacturing technique integrating power grinding with flexible topology modification, which enabled the prediction and active control of gear interface textures, thereby effectively reducing vibration and noise. Additionally, Zhang et al. [119] and Chen et al. [120] respectively explored the nonlinear relationships between texture parameters and debris capture capability, as well as between texture parameters and meshing stiffness, providing a theoretical basis for texture design under complex operating conditions.

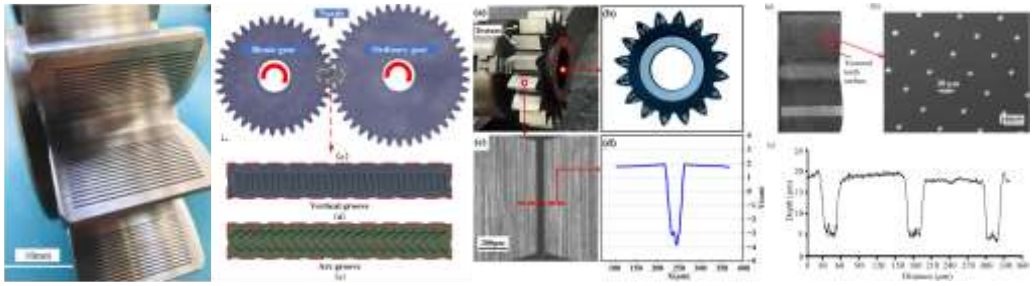

(a) (b) (c) (d)

Figure 6. Different gear meshing interface textures.

The fabrication of high-performance textures relies on manufacturing technologies characterized by high precision, high efficiency, and low damage. Current mainstream processes are categorized into subtractive, additive, and material-transfer types, with subtractive manufacturing being the most widely used. Among subtractive techniques, laser processing, particularly femtosecond laser processing, has emerged as the preferred method due to its high precision and flexibility. By adjusting parameters such as laser power and scanning speed, texture morphology can be precisely controlled and surface hardness enhanced; however, challenges regarding the heat-affected zone and slag must be addressed [121,122]. Chemical etching uses etchants to remove material directionally; it is suitable for mass production and preserves the mechanical properties of the substrate, yet is limited by corrosiveness and processing speed [123–125]. Micro-grinding enables superior surface quality and the fabrication of complex micro-grooves, whereas abrasive flow machining offers excellent uniformity on complex tooth surfaces but presents challenges in shape control [126,127]. Additionally, abrasive water jet machining removes material via high-speed abrasive impingement, offering potential for high efficiency and environmental friendliness [128–130] Conversely, electrical discharge machining, while suitable for hard conductive materials, is associated with issues such as recast layers and low efficiency. Regarding additive techniques, 3D printing (additive manufacturing) can fabricate complex three-dimensional structures but currently faces limitations related to material grain structure and cracking [131,132]. Material transfer techniques, such as micro-texture rolling, leverage plastic deformation to transfer patterns, offering high efficiency and consistency; however, challenges exist when processing high-hardness or complex textures [133]. Wos et al. and Petare et al. [134,135] adopted a process combining laser pre-treatment with abrasive flow machining, which significantly enhanced the quality and wear resistance of the tooth surfaces. Currently, process selection requires careful consideration of material characteristics and costs. Looking ahead, driven by the development of hybrid processes (e.g., laser-

 doi:10.20944/preprints202602.0594.v1

electrochemical combinations, integration of abrasive water jet with milling) and digital control technologies, the manufacturing of gear interface textures is poised to evolve towards greater efficiency and precision.

4.3. Meshing Interface Enriched Lubrication Considering Micro-Texture Effects

To accurately predict and design the lubrication performance of textured gears, theoretical research has evolved from simple isothermal models to complex multi-physics simulations. Early studies were primarily based on isothermal assumptions, focusing on analyzing the influence of texture parameters on lubrication. Li et al. [136] confirmed that increasing the micro-dimple area ratio increases the oil film thickness. Zhao et al. [137] respectively verified the positive effects of grooves and laser textures in enhancing hydrodynamic effects. Furthermore, Petare et al. [138,139] utilized transient EHL theory to investigate the influence of comprehensive curvature radius, entrainment velocity, and load on lubrication states. Morales-Espejel et al. [140] further studied the role of texture orientation. These works laid the foundation for optimizing geometric texture parameters.

As the understanding of lubrication mechanisms has deepened, research has increasingly focused on complex interfacial behaviors and thermo-dynamic coupling effects. Wang et al. [141] revealed the patterns by which interface texture-induced cavitation effects vary with rotational speed, load, and geometric parameters. Xiao et al. [142] established a model that accounts for the coupling between surface roughness and micro-textures, demonstrating that optimizing the aspect ratio can reduce tooth surface stress by approximately 50%, thereby significantly extending fatigue life. Given the pronounced thermal effects under high-speed, heavy-load conditions, current research has shifted towards thermal TEHL and dynamic-coupling models. Liu et al. [143] proposed a three-dimensional thermoelastic-dynamic contact model. Furthermore, Cheng et al. [144] and Ruan et al. [145] utilized mixed lubrication analysis and interface friction-dynamic coupling models, respectively, to reveal the complex influence of textures on contact stiffness, damping, and system vibration, indicating that the interaction between surface roughness and texture is directly related to the dynamic stability and thermal behavior of gear systems.

In light of the complexity inherent in the continuous dynamic process of gear meshing, research trends are shifting from single-point analysis towards multi-scale coupling and system-level simulation. On one hand, micro-texture macro meshing multi-scale coupling analysis has emerged as a prominent research area. This approach embeds local lubrication boundaries that account for texture effects into macroscopic dynamic models, thereby enabling precise mapping between microstructural features and macroscopic motion. On the other hand, research focuses on system-level evaluation, comprehensively considering the influence of textured gear pairs on the transmission's overall efficiency, vibration, noise, and temperature rise. These frontier directions not only deepen the understanding of the underlying mechanisms of textures but also provide critical support for the global optimization of high-performance gear transmission systems; however, their implementation also imposes higher demands on computational capabilities and numerical algorithms.

4.4. Multiscale Micro-Texturing Meshing Interface for Deep-Sea Gear Transmission Environmental Challenge

In recent years, numerous scholars have conducted experimental investigations into the tribological performance of interface textures in marine environments. These studies typically employ experimental setups that simulate marine conditions, such as seawater-lubricated bearing test rigs and high-pressure chamber friction testers, to validate the efficacy of interface textures. A study focusing on marine propeller hub bearings demonstrated that surface texturing technology can significantly enhance tribological performance, reducing the friction coefficient by 20-30% and the wear volume by 40-50%. This improvement is particularly pronounced under starved lubrication conditions, as the textures provide a continuous lubricant supply, thereby reducing the likelihood of direct metal-to-metal contact. Another investigation into the tribological properties of textured

 doi:10.20944/preprints202602.0594.v1

titanium alloys under dry friction and perfluoropolyether oil lubrication found that appropriately designed interface textures can significantly improve the wear resistance of titanium alloys, especially in harsh environments. This is of great significance for titanium alloy gears, which are widely utilized in marine equipment. Furthermore, research has explored the tribological performance of a combined system involving surface texturing and ionic liquid lubrication in marine settings. The results indicated that the two exhibit a synergistic effect, capable of further enhancing the wear and corrosion resistance of gears. This provides novel insights for the development of specialized gear lubrication systems tailored for marine environments.

Although surface texturing technology has demonstrated promising results in laboratory studies, its practical application in marine gear transmission systems faces several challenges, including high fabrication costs, long-term durability, and the impact on gear strength. These issues require further investigation and resolution to facilitate the engineering application of this technology. While current research on gear surface texturing specifically for marine environments is limited, analysis of the underlying mechanisms suggests that interface textures hold immense potential for addressing marine environmental challenges. The oil storage capacity of textures can supply essential lubrication to the meshing zone during the startup phase, characterized by low temperatures, high viscosity, and poor lubricant fluidity, thereby preventing dry friction. Furthermore, when lubricant viscosity decreases due to seawater contamination, the secondary hydrodynamic effect generated by textures can partially compensate for the loss of load-carrying capacity, helping to maintain the necessary oil film thickness. While interface textures themselves do not possess intrinsic corrosion resistance, they provide a physical carrier for integrating anti-corrosion and friction-reduction technologies. Conversely, a purely textured surface may even accelerate localized corrosion due to the increased surface area and the formation of occluded cells. Therefore, it is essential to consider surface texturing and anti-corrosion coating technologies in synergy.

5. Conclusions and Prospects

This study presents a systematic review of how the distinctive and harsh marine environment, characterized by extreme hydrostatic pressure and cryogenic temperatures, influences the lubrication performance of gear transmission systems. Centered on EHL theory and surface micro-texturing technology, it synthesizes recent research advances, identifies critical scientific gaps, and outlines key technical challenges in deep-sea tribological applications.

5.1. Summary of Findings and Conclusions

The marine environment, characterized by high pressure and low temperature, poses multiple challenges for gear lubrication by significantly altering the viscosity-pressure, viscosity-temperature, density, and thermophysical properties of lubricants. The ultra-high viscosity resulting from the coupling of high pressure and low temperature is a core issue, leading to problems such as poor fluidity, difficult startup, high churning losses, and lubricant starvation. Furthermore, the risks of emulsification, corrosion, and additive failure associated with seawater intrusion further exacerbate the likelihood of lubrication failure.

EHL theory has effectively guided the design of gear lubrication systems. However, the drastic temperature and pressure changes in extreme deep-sea environments render the viscosity-pressure characteristics, rheological behavior, and thermal effects of lubricants non-negligible, prompting the evolution of gear EHL theory towards TEHL. Although current TEHL research has established transient numerical models coupling thermal effects, non-Newtonian rheology, and realistic surface topography, simulation studies specifically targeting deep-sea high-pressure and low-temperature environments remain limited. The primary bottlenecks are the lack of lubricant property data under extreme operating conditions and numerical convergence challenges arising from multi-field coupling.

Interface texture technology effectively enhances the storage, flow, and load-carrying capacity of lubricants by fabricating microstructures on the gear surface, thereby reducing gear friction and

 doi:10.20944/preprints202602.0594.v1

wear. Optimal interface texture design can significantly improve the tribological performance of gears under mixed and boundary lubrication conditions, making it theoretically suitable for addressing challenges such as low-temperature startup and low-speed heavy-load operations in deep-sea gears. However, to fully harness the potential of interface textures, it is necessary to optimize their parameters for specific operating conditions and address long-term reliability issues in deep-sea environments.

5.2. Future Research Perspectives

Despite significant progress in research on deep-sea gear transmission lubrication, existing theories and technologies still face numerous bottlenecks under the combined challenges of extremely high pressure, low temperature, and severe corrosion, necessitating further in-depth exploration.

High pressure and low temperature significantly alter the physical properties of lubricants. At the same time, seawater corrosion fundamentally undermines both lubricant performance and tooth surface integrity, posing a risk of failure to traditional TEHL theory. Currently, detailed mechanistic studies on how seawater corrosion affects the TEHL oil film thickness, pressure distribution, and temperature fields are scarce. Furthermore, there is a lack of systematic understanding regarding the evolutionary patterns of gear material wear and lubricant aging under multi-field coupling. Theoretical research on synergistic design, optimization methods, and case studies of gear interface textures and anti-corrosion coatings is limited, with applications in high-pressure, low-temperature marine environments still in their infancy. Additionally, laboratory simulations struggle to fully replicate actual deep-sea operating conditions, meaning the long-term durability of integrated texture-coating surfaces and their impact on system dynamic characteristics require further verification. To date, no comprehensive literature exists that integrates TEHL, interface textures, anti-corrosion coatings, and specialty lubricants to provide a complete technical framework for addressing these issues.

As marine equipment evolves toward greater depths and extended mission endurance, future research should focus on developing multi-physics coupling simulation models to achieve precise prediction and optimization of the corrosion-coating-texture-lubrication system. It is essential to establish high-fidelity experimental testing platforms, combined with in-situ long-term monitoring and real-time condition sensing technologies, to provide reliable data support for new materials and designs. Concurrently, by integrating multidisciplinary technologies from materials science, fluid mechanics, and data science, the engineering application of lubricants and integrated texture-coating manufacturing processes should be promoted, ultimately achieving high reliability and long service life for gear transmission systems in marine environments.

Author Contributions: Conceptualization, X. W. and Y. W.; methodology, W. Z.; software, J. R.; validation, X. W., Y. W. and J. R.; formal analysis, X. W.; investigation, J. R.; resources, Y. W.; data curation, W. Z.; writing—original draft preparation, W. Z. and X. W.; writing—review and editing, X. W., Y. W. and J. R.; visualization, J. R.; supervision, J. R. and W. Z.; project administration, Y. W. and W. Z. All authors have read and agreed to the published version of the manuscript.

Funding: The research subject was supported by the National Natural Science Foundation Sponsored Project (Project Approval Number: 52475257), the National Key Research and Development Program Project (Grant No. 2023YFB3406301), the Fund Project for Technological Field of National Defense Science and Technology Plan 173 (2024-JCJQ-JJ-2020) and (2024-JCJQ-JJ-2043), the Marine Propulsion Research and Development (MPRD) Program (Grant No. MG20220203).

Institutional Review Board Statement: Not applicable.

Informed Consent Statement: Not applicable.

Data Availability Statement: Not applicable.

 doi:10.20944/preprints202602.0594.v1

Acknowledgments: The authors would like to thank the Huaqiao University (HQU), Heilongjiang Institute of Technology (HLJIT), and the Harbin Institute of Technology (HIT) for their support.

Conflicts of Interest: No conflict of interest exits in the submission of this manuscript, and manuscript is approved by all authors for publication. We would like to declare on behalf of our co-authors that the work described was original research that has not been published previously, and not under consideration for publication elsewhere, in whole or in part. All the authors listed have approved of the manuscript that is enclosed.

References

1. Brandt, A.; Gutt, J.; Hildebrandt, M.; Pawlowski, J.; Schwendner, J.; Soltwedel, T.; Thomsen, L. Cutting the umbilical: new technological perspectives in benthic deep-sea research. *Journal of Marine Science and Engineering* **2016**, *4*, 36.
2. Zhang, T.; Wang, R.; Wang, Y.; Cheng, L.; Wang, S.; Tan, M. Design and locomotion control of a dactylopteridae-inspired biomimetic underwater vehicle with hybrid propulsion. *IEEE Transactions on Automation Science and Engineering* **2021**, *19*, 2054-2066.
3. Gao, H.; Wu, D.; Gao, C.; Xu, C.; Yang, X. Development of a six-degree-of-freedom deep-sea water-hydraulic manipulator. *Journal of Marine Science and Engineering* **2024**, *12*, 1696.
4. He, Y.; Chen, C.; Bu, C.; Han, J. A polar rover for large-scale scientific surveys: design, implementation and field test results. *International Journal of Advanced Robotic Systems* **2015**, *12*, 145.
5. Ruan, J.; Wang, X.; Wang, Y.; Zou, W. Mechanistic Analysis of Textured IEL and Meshing ASLBC Synergy in Heavy Loads: Characterizing Predefined Micro-Element Configurations. *Machines* **2025**, *13*, 842.
6. Cao, W., Yu, Z., Yang, G., Li, X., Wang A.: Study on the Evolution of Volume Efficiency of Gear Pump in Deep Sea Extreme Environment. *Chinese Hydraulics & Pneumatics*, **2024**, *48*, 28-36.
7. Mia, S.; Mizukami, S.; Fukuda, R.; Morita, S.; Ohno, N. High-pressure behavior and tribological properties of wind turbine gear oil. *Journal of mechanical science and technology* **2010**, *24*, 111-114.
8. Du, K.; Xi, W.; Huang, S.; Zhou, J. Deep-sea mineral resource mining: a historical review, developmental progress, and insights. *Mining, Metallurgy & Exploration* **2024**, *41*, 173-192.
9. Shen, Y.; Chen, M.; Du, Y.; Li, M. Key mechanical issues and technical challenges of deep-sea mining development system. *Mechanics in Engineering* **2022**, *44*, 1005-1020.
10. Zhao, Y.; Li, N.; Xie, K.; Wang, C.; Zhou, S.; Zhang, X.; Ye, C. Manufacturing of lithium battery toward deep-sea environment. *International Journal of Extreme Manufacturing* **2024**, *7*, 022009.
11. Song, W.; Cui, W. An overview of underwater connectors. *Journal of marine science and engineering* **2021**, *9*, 813.
12. Chen, Z.; Dai, Y.; Wu, S.; Yang, C. Active Pressure-Compensation Technology for Deep-Sea Fluid Samplers. *IEEE Journal of Oceanic Engineering* **2025**, *50*, 2456-2467.
13. Sperka, P.; Krupka, I.; Hartl, M. Lubricant flow in thin-film elastohydrodynamic contact under extreme conditions. *Friction* **2016**, *4*, 380-390.
14. Cai, M.; Wu, S.; Yang, C. Effect of low temperature and high pressure on deep-sea oil-filled brushless DC motors. *Marine Technology Society Journal* **2016**, *50*, 83-93.
15. Li, R.; Shi, X.; Lu, X.; Sun, W.; Liu, H. Study on Mixed Lubrication Characteristics of Helical Gears of Marine Diesel Engine under Real Machining Surface. *Journal of Mechanical Engineering* **2025**, *61*, 290-304.
16. Gong, P.; Wen, X.; Bai, P.; Yue, L.; Ding, J.; Tian, Y.; Li, L. Influence of Low Concentration Seawater on the Friction Corrosion Performance of Water–Glycol Fire-Resistant Hydraulic Fluid. *Journal of Bio-and Tribo-Corrosion* **2024**, *10*, 49.
17. Chen, B.; Wang, J.; Yan, F. Friction and wear behaviors of several polymers sliding against GCr15 and 316 steel under the lubrication of sea water. *Tribology letters* **2011**, *42*, 17-25.
18. Xiao, D.; Deng, Y.; Wang, Z.; Li, T.; Liu, Y. Viscosity evolution of water glycol in deep-sea environment at high pressure and low temperature. *Journal of Molecular Liquids* **2023**, *387*, 122387.
19. Qian, X.; Yan, W.; Chen, S.; Zhang, Y.; Luo, Y.; Liu, C. Optimization of splash lubrication in the gearbox considering heat transfer performance. *Tribology International* **2024**, *195*, 109592.

 doi:10.20944/preprints202602.0594.v1

20. Tošić, M.; Larsson, R.; Stahl, K.; Lohner, T. Thermal elastohydrodynamic analysis of a worm gear. *Machines* **2023**, *11*, 89.
21. Wu, J.; He, T.; Wang, D.; Wang, L.; Jiang, S.; Wang, Y.; Chen, K.; Zhang, C.; Shu, K.; Li, Z. Transient mixed thermal elastohydrodynamic lubrication analysis of aero ball bearing under non-steady state conditions. *Tribology International* **2025**, *202*, 110342.
22. Lv, F.; Zhang, X.; Ji, C.; Rao, Z. Theoretical and experimental investigation on local turbulence effect on mixed-lubrication journal bearing during speeding up. *Physics of Fluids* **2022**, *34*, 113104.
23. Torres, T.; Changenet, C.; Touret, T.; Guilbert, B. A new experimental methodology to study convective heat transfer in oil jet lubricated gear units. *Lubricants* **2023**, *11*, 408.
24. Zhang, S.; Zhang, C. A new deterministic model for mixed lubricated point contact with high accuracy. *Journal of Tribology* **2021**, *143*, 102201.
25. Jian, G.; Wang, Y.; Luo, H.; Li, Y. Thermal Elastohydrodynamic Lubrication of X-Gears System Based on Time-Varying Meshing Stiffness. *Tribology* **2020**, *40*, 21-29.
26. Yuan, C.; Shen, R.; Dai, Q.; Huang, W.; Wang, X. Influence of Surface Texture on the Isothermal Elastohydrodynamic Lubrication Performance of Gears. *Tribology* **2025**, *45*, 1033-1046.
27. Tortorella, E.; Tedesco, P.; Palma Esposito, F.; January, G.G.; Fani, R.; Jaspars, M.; De Pascale, D. Antibiotics from deep-sea microorganisms: current discoveries and perspectives. *Marine drugs* **2018**, *16*, 355.
28. Skropeta, D.; Wei, L. Recent advances in deep-sea natural products. *Natural product reports* **2014**, *31*, 999-1025.
29. Amano, C.; Zhao, Z.; Sintes, E.; Reinthaler, T.; Stefanschitz, J.; Kisadur, M.; Utsumi, M.; Herndl, G. J. Limited carbon cycling due to high-pressure effects on the deep-sea microbiome. *Nature Geoscience* **2022**, *15*, 1041-1047.
30. Peacock, T.; Ouillon, R. The fluid mechanics of deep-sea mining. *Annual Review of Fluid Mechanics* **2023**, *55*, 403-430.
31. Scheffer, G.; Gieg, L. M. The mystery of piezophiles: Understudied microorganisms from the deep, dark subsurface. *Microorganisms* **2023**, *11*, 1629.
32. Wang, Y. N.; Meng, L. H.; Wang, B. G. Progress in research on bioactive secondary metabolites from deep-sea derived microorganisms. *Marine Drugs* **2020**, *18*, 614.
33. Paul, V. J.; Ritson-Williams, R.; Sharp, K. Marine chemical ecology in benthic environments. *Natural product reports* **2011**, *28*, 345-387.
34. Sun, D.; Wang, C. A review of open ocean zooplankton ecology. *Acta Ecologica Sinica* **2017**, *37*, 3219-3231.
35. Wood, R. J. K. Marine wear and tribocorrosion. *Wear* **2017**, *376*, 893-910.
36. Von der Ohe, C. B.; Johnsen, R.; Espallargas, N. Modeling the multi-degradation mechanisms of combined tribocorrosion interacting with static and cyclic loaded surfaces of passive metals exposed to seawater. *Wear* **2010**, *269*, 607-616.
37. Himanshu, G.; Tauheed, M.; Pradeep, K. Review of condition monitoring approaches for ball screws. *Advanced Engineering Informatics* **2026**, *71*, 104206.
38. Bair, S. S.; Andersson, O.; Qureshi, F. S.; Schirru, M. M. New EHL modeling data for the reference liquids squalane and squalane plus polyisoprene. *Tribology Transactions* **2018**, *61*, 247-255.
39. Boussaid, M.; Haddadine, N.; Benmounah, A.; Dahal, J.; Bouslah, N.; Benaboura A.; El-Shall, S. Viscosity-boosting effects of polymer additives in automotive lubricants. *Polymer Bulletin* **2024**, *81*, 6995-7011.
40. Su, R.; Cao, W.; Jin, Z.; Wang, Y.; Ding, L.; Maqsood, M.; Wang, D. Deterioration Mechanism and Status Prediction of Hydrocarbon Lubricants under High Temperatures and Humid Environments. *Lubricants* **2024**, *12*, 116.
41. Xu, R.; Martinie, L.; Vergne, P.; Joly, L.; Fillo, N. An Approach for Quantitative EHD Friction Prediction Based on Rheological Experiments and Molecular Dynamics Simulations. *Tribology Letters* **2023**, *71*, 69.
42. Zhang, X.; Yu, T.; Ji, H.; Guo, F.; Duan, W.; Liang, P.; Ma, L. Analysis of Water-Lubricated Journal Bearings Assisted by a Small Quantity of Secondary Lubricating Medium with Navier–Stokes Equation and VOF Model. *Lubricants* **2024**, *12*, 16.
43. Seeton, C. J. Viscosity-temperature correlation for liquids. *Tribology Letters* **2006**, *22*, 67-78.

 doi:10.20944/preprints202602.0594.v1

44. Levit, R.; Martinez-Garcia, J. C.; Ochoa, D. A.; García, J. The generalized Vogel-Fulcher-Tamman equation for describing the dynamics of relaxer ferroelectrics. *Scientific Reports* **2019**, *9*, 12390.
45. Bair, S. The unresolved definition of the pressure-viscosity coefficient. *Scientific Reports* **2022**, *12*, 3422.
46. Andersson, H.; Holmberg, L. J.; Simonsson, K.; Hilding, D.; Schill, M.; Borrvall, T.; Sigfridsson, E.; Leidermark, D. Simulation of leakage flow through dynamic sealing gaps in hydraulic percussion units using a co-simulation approach. *Simulation Modelling Practice and Theory* **2021**, *111*, 102351.
47. Lei, M.; Yu, K.; Lu, H.; Qi, H. J. Influence of structural relaxation on thermomechanical and shape memory. *Polymer* **2017**, *109*, 216-228.
48. Gupta, P. K.; Taketa, J.; Price, C. M. Thermal interactions in rolling bearings. *Proceedings of the Institution of Mechanical Engineers, Part J: Journal of Engineering Tribology* **2020**, *234*, 1233-1253.
49. Ewen, J. P.; Heyes, D. M.; Dini, D. Advances in nonequilibrium molecular dynamics simulations of lubricants and additives. *Friction* **2018**, *6*, 349-386.
50. Xu, C.; Schall, D.; Barber, G. Molecular dynamics simulation on the friction properties of confined nanofluids. *Materials Today Communications* **2023**, *34*, 105252.
51. Hartung, H. A. Density-Temperature-Pressure Relations for Liquid Lubricants. *Journal of Fluids Engineering* **2022**, *78*, 941-946.
52. Zhou, Z.; Zhou, X.; Huang, Q.; Liu, X.; Wang, L.; Xing, S. Impact of oil-water emulsions on lubrication performance of ship stern bearings. *Scientific Reports* **2024**, *14*, 31478.
53. Harika, E.; Jarny, S.; Monnet, P.; Bouyer, J.; Fillon, M. Effect of water pollution on rheological properties of lubricating oil. *Applied Rheology* **2011**, *21*, 12613.
54. Ouyang, W.; Yan, Z.; Zhou, X.; Luo, B.; Wang, B.; Huang, J. A thermal hydrodynamic model for emulsified oil-lubricated tilting-pad thrust bearings. *Lubricants* **2023**, *11*, 529.
55. Tian, Y.; Zhou, J.; He, C.; He, L.; Li, X.; Sui, H. The formation, stabilization and separation of oil-water emulsions: a review. *Processes* **2022**, *10*, 738.
56. Wang, J.; Chen, J.; Chen, B.; Yan, F.; Xue, Q. Wear behaviors and wear mechanisms of several alloys under simulated deep-sea environment covering seawater hydrostatic pressure. *Tribology International* **2012**, *56*, 38-46.
57. Liu, Y.; Ma, G.; Ma, X.; Li, H.; Guo, P.; Wang, A.; Ke, P. Corrosion and tribocorrosion performance degradation mechanism of multilayered graphite-like carbon (GLC) coatings under deep-sea immersion in the western Pacific. *Corrosion Science* **2024**, *239*, 112418.
58. Ijaz Malik, M. A.; Kalam, M. A.; Mujtaba, M. A.; Almomani, F. A review of recent advances in the synthesis of environmentally friendly, sustainable, and nontoxic bio-lubricants: Recommendations for the future implementations. *Environmental Technology & Innovation* **2023**, *32*, 103366.
59. Litwin, W.; Barszczewska, A.; Piątkowska, E.; Szwoch, I.; Matuszewski, L.; Kahsin, M. Influence of lubrication water contamination by solid particles of mineral origin on marine strut propeller shafts bearings of ships. *Polish Maritime Research* **2024**, *31*, 187-196.
60. Hossain, M. A.; Iqbal, M. A. M.; Julkapli, N. M.; Kong, P. S.; Ching, J. J.; Lee, H. V. Development of catalyst complexes for upgrading biomass into ester-based biolubricants for automotive applications: a review. *RSC advances* **2018**, *8*, 5559-5577.
61. Gonon, M.; Philippon, D.; Margueritat, J.; Lafarge, L.; Vergne, P.; Martinie, L. New Insight into the Correlation Between Lubricant Glass Transition and friction Plateau in Highly Loaded Contacts. *Tribology Letters* **2025**, *73*, 150.
62. Bair, S. The viscosity at the glass transition of a liquid lubricant. *Friction* **2019**, *7*, 86-91.
63. Conrad, A.; Hodapp, A.; Hochstein, B.; Willenbacher, N.; Jacob, K. H. Low-temperature rheology and thermoanalytical investigation of lubricating oils: Comparison of phase transition, viscosity, and pour point. *Lubricants* **2021**, *9*, 99.
64. Cui, W.; Chen, H.; Zhao, J.; Ma, Q.; Xu, Q.; Ma, T. Progresses on cryo-tribology: lubrication mechanisms, detection methods and applications. *International Journal of Extreme Manufacturing* **2023**, *5*, 022004.
65. Li, T.; Yang, Y.; Zhang, Y.; Zhao, C. Online Friction-Thermal-Load Coupling Model of an Arbitrary Curve Contact Under Mixed Lubrication Considering Actual Operating Conditions. *Journal of Tribology* **2022**, *144*, 112201.

 doi:10.20944/preprints202602.0594.v1

66. Chong, W. W. F.; Hamdan, S. H.; Wong, K. J.; Yusup, S. Modelling transitions in regimes of lubrication for rough surface contact. *Lubricants* **2019**, *7*, 77.
67. Kumar, R.; Hussain ova, I.; Rahmani, R.; Antonov, M. Solid lubrication at high-temperatures-A review. *Materials* **2022**, *15*, 1695.
68. Gorbacheva, S. N.; Yadykova, A. Y.; Ilyin, S. O. Rheological and tribological properties of low-temperature greases based on cellulose acetate butyrate gel. *Carbohydrate Polymers* **2021**, *272*, 118509.
69. Maier, E.; Ziegltrum, A.; Lohner, T.; Stahl, K. Characterization of TEHL contacts of thermoplastic gears. *Forschung im Ingenieurwesen* **2017**, *81*, 317-324.
70. Liu, Y. Y.; Li, Y. R.; Wang, L. Q. Experimental and theoretical studies on the pressure fluctuation of an internal gear pump with a high pressure. *Proceedings of the Institution of Mechanical Engineers, Part C: Journal of Mechanical Engineering Science* **2019**, *233*, 987-996.
71. Xiao, Z.; Li, Z.; Shi, X.; Zhou, C. Oil Film Damping Analysis in Non-Newtonian Transient Thermal Elastohydrodynamic Lubrication for Gear Transmission. *Journal of Applied Mechanics* **2018**, *85*, 035001.
72. Duan, Z.; Wu, T.; Glowacz, A.; Gupta, M. K.; Królczyk, G. Analysis of the line contact tribo-lubrication pair and failure mechanism under the extreme conditions. *Tribology International* **2023**, *185*, 108505.
73. Yin, Z.; Fan, Z.; Jiang, F. Oil film stiffness of double involute gears based on thermal EHL theory. *Chinese journal of mechanical engineering* **2021**, *34*, 60.
74. Wang, Z.; Dong, Q.; Shi, X.; Bai, X.; Li, T. An Investigation Into the Thermal Behavior of Planetary Gear Systems Under Mixed Lubrication. *Journal of Tribology* **2026**, *148*, 042204.
75. Su, B.; Mao, S.; Zhang, G.; Li, H.; Cui, Y. Dynamics-Based Calculation of the Friction Power Consumption of a Solid Lubricated Bearing in an Ultra-Low Temperature Environment. *Lubricants* **2023**, *11*, 372.
76. Liu, Y.; Wang, B.; Yang, S.; Liao, Y.; Guo, T. Characteristic analysis of mechanical thermal coupling model for bearing rotor system of high-speed train. *Applied Mathematics and Mechanics* **2022**, *43*, 1381-1398.
77. Wang, L.; Zhao, Q.; Feng, W.; Xiang, G. On the Film Stiffness Characteristics of Water-Lubricated Rubber Bearings in Deep-Sea Environments. *Lubricants* **2025**, *13*, 451.
78. Ziegltrum, A.; Lohner, T.; Stahl, K. TEHL simulation on the influence of lubricants on the frictional losses of DLC coated gears. *Lubricants* **2018**, *6*, 17.
79. Sivayogan, G.; Rahmani, R.; Rahnejat, H. Lubricated loaded tooth contact analysis and non-Newtonian thermoelastohydrodynamics of high-performance spur gear transmission systems. *Lubricants* **2020**, *8*, 20.
80. Mounayer, J.; Habchi, W. Exact model order reduction for the full-system finite element solution of thermal elastohydrodynamic lubrication problems. *Lubricants* **2023**, *11*, 61.
81. Yin, Z.; Fan, Z.; Wang, M. Thermal elastohydrodynamic lubrication characteristics of double involute gears at the graded position of tooth waist. *Tribology Internationa*l **2020**, *144*, 106028.
82. MacLaren, A.; Kadiric, A. Elastohydrodynamic Traction and Film Thickness at High Speeds. *Tribology Letters* **2024**, *72*, 92.
83. Li, B.; Mao, Z.; Song, B.; Tian, W.; Wang, Y.; Sundén, B.; Lu, C. Thermal management performance improvement of phase change material for autonomous underwater vehicles' battery module by optimizing fin design based on quantitative evaluation method. *International Journal of Energy Research* **2022**, *46*, 15756-15772.
84. Castaño, T. P.; Velázquez, J. J. L. On the dynamics of thin layers of viscous flows inside another viscous fluid. *Journal of Differential Equations* **2021**, *300*, 252-311.
85. Kolivand, A.; Li, S.; Zhang, Q. Modeling on contact fatigue under starved lubrication condition. *Meccanica* **2021**, *56*, 211-225.
86. Zhao, E.; Shao, B.; Qiao, M.; Quan, L.; Wang, C. Influence of Temperature Rise on Local Lubrication and Friction Characteristics of Wet Clutch. *Tribology* **2024**, *44*, 831-841.
87. Fang, J.; Cao, H.; Bai, P.; Meng, Y.; Ma, L.; Tian, Y. High-pressure rheological properties of polyalphaolefin and ester oil blends and their impact on lubrication. *Tribology International* **2025**, *201*, 110262.
88. Wang, Z.; Pu, W.; He, T.; Wang, J.; Cao, W. Numerical simulation of transient mixed elastohydrodynamic lubrication for spiral bevel gears. *Tribology International* **2019**, *139*, 67-77.

 doi:10.20944/preprints202602.0594.v1

89. Shi, X.; Lu, X.; He, T.; Sun, W.; Tong, Q.; Ma, X.; Zhao, B.; Zhu, D. Predictions of friction and flash temperature in marine gears based on a 3D line contact mixed lubrication model considering measured surface roughness. *Journal of Central South University* **2021**, *28*, 1570-1583.
90. Amine, G.; Fillot, N.; Philippon, D.; Devaux, N.; Dufils, J.; Macron, E. Dual experimental-numerical study of oil film thickness and friction in a wide elliptical TEHL contact: From pure rolling to opposite sliding. *Tribology International* **2023**, *184*, 108466.
91. Saxena, A.; Jacobs, G.; König, F.; Reimers, M. Influences of contact parameters on the wear-protective boundary layer formation in rolling-sliding contacts. *Wear* **2025**, *580-581*, 206259.
92. Ruan, J.; Wang, X.; Wang, Y.; Zou, W. Multiscale Fractal Analysis of Thermo-Mechanical Coupling in Textured Tribological Interfaces. *Symmetry* **2025**, *17*, 1799.
93. Zhou, Z.; Chen, D.; Yuan, C.; Dai, Q.; Huang, W.; Wang, X. State of Art in Tribological Design and Surface Texturing of Gear Surfaces. *China Surface Engineering* **2024**, *37*, 61-78.
94. Xu, J.; Lu, H.; Cai, L.; Liao, Y.; Lian, J. Surface protection technology for metallic materials in marine environments. *Materials* **2023**, *16*, 6822.
95. Braumann, L.; de Viteri, V. S.; Morhard, B.; Lohner, T.; Ochoa, J.; Amri, H. Tribology technologies for gears in loss of lubrication conditions: a review. *Journal of Materials Science: Materials in Engineering* **2025**, *20*, 29.
96. Arumugaprabu, V.; Ko, T. J.; Kumaran, T.; Kurniawan, R.; Uthayakumar, M. A brief review on importance of surface texturing in materials to improve the tribological performance. *Reviews on Advanced Materials Science* **2018**, *53*, 40-48.
97. Watanabe, I. A.; Okubo, H.; Nakano, K. In-situ electrical impedance observation for lubrication conditions of gears under actual operation. *Tribology International* **2025**, *210*, 110777.
98. Chen, K.; Yang, X.; Zhang, Y.; Yang, H.; Lv, G.; Gao, Y. Research progress of improving surface friction properties by surface texture technology. *The International Journal of Advanced Manufacturing Technology* **2021**, *116*, 2797-2821.
99. Guo, Q.; Zheng, L.; Zhong, Y.; Wang, S.; Ren, L. Numerical simulation of hydrodynamic lubrication performance for continuous groove-textured surface. *Tribology International* **2022**, *167*, 107411.
100. Gropper, D.; Wang, L.; Harvey, T. J. Hydrodynamic lubrication of textured surfaces: A review of modeling techniques and key findings. *Tribology international* **2016**, *94*, 509-529.
101. Wang, W. H.; Yuan, W.; Guo, Q. J.; Chi, B. T.; Yin, F. S.; Wang, N. N.; Yu, J. Tribological properties of ductile cast iron with in-situ textures created through abrasive grinding and laser surface ablation. *Tribology International* **2024**, *200*, 110134.
102. Yin, H.; Zhang, X.; Guo, Z.; Xu, Y.; Rao, X.; Yuan, C. Synergetic effects of surface textures with modified copper nanoparticles lubricant additives on the tribological properties of cylinder liner-piston ring. *Tribology International* **2023**, *178*, Part A, 108085.
103. Vishnoi, M.; Kumar, P.; Murtaza, Q. Surface texturing techniques to enhance tribological performance: A review. *Surfaces and Interfaces* **2021**, *27*, 101463.
104. Shen, Z. H.; Wang, F. C.; Chen, Z. G.; Ruan, X. P.; Zeng, H. H.; Wang, J. H.; An, Y. R.; Fan, X. L. Numerical simulation of lubrication performance on chevron textured surface under hydrodynamic lubrication. *Tribology International* **2021**, *154*, 106704.
105. Mao, B.; Siddaiah, A.; Liao, Y. L.; Menezes, P. L. Laser surface texturing and related techniques for enhancing tribological performance of engineering materials: A review. *Journal of Manufacturing Processes* **2020**, *53*, 153-173.
106. Maldonado-Cortés, D.; Peña-Parás, L.; Martínez, N. R.; Leal, M. P.; Correa, D. I. Q. Tribological characterization of different geometries generated with laser surface texturing for tooling applications. *Wear* **2021**, *477*, 203856.
107. Moradi, M.; Arabi, H.; Nasab, S. J.; Benyounis, K. Y. A comparative study of laser surface hardening of AISI 410 and 420 martensitic stainless steels by using diode laser. *Optics & Laser Technology* **2019**, *111*, 347-357.
108. Wang, Z.; Ye, R.; Xiang, J. The performance of textured surface in friction reducing: A review. *Tribology International* **2023**, *177*, 108010.

 doi:10.20944/preprints202602.0594.v1

109. Chang, X.; Renqing, D.; Liao, L.; Zhu, P.; Lin, B.; Huang, Y.; Luo, S. Study on hydrodynamic lubrication and friction reduction performance of spur gear with groove texture. *Tribology International* **2023**, *177*, 107978.
110. Lei, P. X.; Zhang, P. L.; Song, S. J.; Liu, Z. Y.; Yan, H.; Sun, T. Z.; Lu, Q. H.; Chen, Y.; Gromov, V.; Shi, H. C. Research status of laser surface texturing on tribological and wetting properties of materials: A review. *Optik* **2024**, *298*, 171581.
111. Zhang, Z.; Li, J.; Zou, T.; Hou, W.; An, Y.; Liu, J. Effect of bionic texture on wear resistance and heat dissipation performance of transmission gear. *Tribology Transactions* **2025**, *68*, 531-557.
112. Wang, Y.; Luo, S.; Gao, T.; Mo, J.; Wang, D.; Chang, X. Biomimetic Hexagonal Texture with Dual-Orientation Groove Interconnectivity Enhances Lubrication and Tribological Performance of Gear Tooth Surfaces. *Lubricants* **2025**, *13*, 420.
113. Wang, Z.; Wang, S.; Wang, S.; Xiao, Y.; Dong, J.; Xuan, Y.; Zhang, L.; Wang, H. Study on the Influence of Tooth Surface Micro-texture on Dynamic Characteristics of Face Gear. *Advances in Mechanical Transmission: Innovations and Applications* **2026**, 798-809. (icmt-2 2025. Lecture Notes in Mechanical Engineering. Springer, Singapore.)
114. Zhao, T.; Wang, Y.; He, Y.; Zhu, Y.; Li, M. Numerical simulation and experimental investigation on tribological properties of gear alloy surface biomimetic texture. *Tribology Transactions* **2023**, *66*, 610-622.
115. Gupta, N.; Tandon, N.; Pandey, R. K. An exploration of the performance behaviors of lubricated textured and conventional spur gearsets. *Tribology International* **2018**, *128*, 376-385.
116. Gupta, N.; Tandon, N.; Pandey, R. K.; Vidyasagar, K. E. C.; Kalyanasundaram, D. Tribological and vibration studies of textured spur gear pairs under fully flooded and starved lubrication conditions. *Tribology Transactions* **2020**, *63*, 1103-1120.
117. Gupta, N.; Tandon, N.; Pandey, R. K.; Vidyasagar, K. E. C.; Kalyanasundaram, D. Tribodynamic studies of textured gearsets lubricated with fresh and MoS2 blended greases. *Tribology International* **2022**, *165*, 107247.
118. Tang, J. P.; Han, J.; Tian, X. Q.; Li, Z. F.; You, T. F.; Li, G. H.; Xia, L. Flexible modification and texture prediction and control method of internal gearing power honing tooth surface. *Advances in Manufacturing* **2024**, *13*, 784-798.
119. Zhang, B.; Sun, L.; Zhao, N.; Li, J. Applications of laser surface treatment in gears: a review. *Journal of Materials Engineering and Performance* **2025**, *34*, 1-35.
120. Chen, Z.; Zhou, J.; Liu, B.; Fu, H.; Meng, X.; Ji, J.; Zhang, Y.; Hua, X.; Xu, X.; Fu, Y. Meshing frictional characteristics of spur gears under dry friction and heavy loads: Effects of the preset pitting-like micro-textures array. *Tribology International* **2023**, *180*, 108296.
121. Sharma, R.; Pradhan, S.; Bathe, R. N. Design and fabrication of honeycomb micro-texture using femtosecond laser machine. *Materials and Manufacturing Processes* **2021**, *36*, 1314-1322.
122. Salguero, J.; Del Sol, I.; Vazquez-Martinez, J. M.; Schertzer, M. J.; Iglesias, P. Effect of laser parameters on the tribological behavior of Ti6Al4V titanium microtextures under lubricated conditions. *Wear* **2019**, *426-427*, Part B, 1272-1279.
123. Xu, Y.; Yu, J.; Geng, J.; Abuflaha, R.; Olson, D.; Hu, X.; Tysoe, W. T. Characterization of the tribological behavior of the textured steel surfaces fabricated by photolithographic etching. *Tribology Letters* **2018**, *66*, 55.
124. Xu, Y.; Zheng, Q.; Abuflaha, R.; Olson, D.; Furlong, O.; You, T.; Zhang, Q.; Hu, X.; Tysoe, W. T. Influence of dimple shape on tribofilm formation and tribological properties of textured surfaces under full and starved lubrication. *Tribology International* **2019**, *136*, 267-275.
125. Brăileanu, P. I.; Mocanu, M.-T.; Dobrescu, T. G.; Pascu, N. E.; Dobrotă, D. Structure and Texture Synergies in Fused Deposition Modeling (FDM) Polymers: A Comparative Evaluation of Tribological and Mechanical Properties. *Polymers* **2025**, *17*, 2159.
126. Zhou, W.; Tang, J.; Rong, K.; Li, Z.; Shao, W. A parametric evaluation model of abrasive interaction for predicting tooth rough surface in spiral bevel gear grinding. *Journal of Manufacturing Processes* **2024**, *132*, 659-676.

 doi:10.20944/preprints202602.0594.v1

127. Fu, Y.; Gao, H.; Yan, Q.; Wang, X.; Wang, X. An efficient approach to improving the finishing properties of abrasive flow machining with the analyses of initial surface texture of workpiece. *The International Journal of Advanced Manufacturing Technology* **2020**, *107*, 2417-2432.
128. Jagadish, Bhowmik, S.; Ray, A. Prediction of surface roughness quality of green abrasive water jet machining: a soft computing approach. *Journal of Intelligent Manufacturing* **2019**, *30*, 2965-2979.
129. Natarajan, Y.; Murugesan, P. K.; Mohan, M.; Ali Khan, S. A. L. Abrasive Water Jet Machining process: A state of art of review. *Journal of Manufacturing Processes* **2020**, *49*, 271-322.
130. Shi, L.; Fang, Y.; Dai, Q.; Huang, W.; Wang, X. Surface texturing on SiC by multiphase jet machining with microdiamond abrasives. *Materials and Manufacturing Processes* **2017**, *33*, 1415-1421.
131. Hong, Y.; Zhang, P.; Lee, K. H.; Lee, C. H. Friction and wear of textured surfaces produced by 3D printing. *Science China Technological Sciences* **2017**, *60*, 1400-1406.
132. Naat, N.; Boutar, Y.; Mezlini, S.; de Silva, L. F. M.; Alrasheedi, N. H.; Hajlaoui, K. Study of the effect of bio-inspired surface texture on the shear strength of bonded 3D-printed materials: Comparison between stainless steel and polycarbonate joints. *International Journal of Adhesion and Adhesives* **2024**, *131*, 103658.
133. Li, S.; Parmar, U. The Effects of Microdimple Texture on the Friction and Thermal Behavior of a Point Contact. *ASME. J. Tribol.* **2018**, *140*, 041503.
134. Wos, S.; Koszela, W.; Pawlus, P. Comparing tribological effects of various chevron-based surface textures under lubricated unidirectional sliding. *Tribology International* **2020**, *146*, 106205.
135. Petare, A.; Deshwal, G.; Palani, I. A; Jain, N. K. Laser texturing of helical and straight bevel gears to enhance finishing performance of AFF process. *The International Journal of Advanced Manufacturing Technology* **2020**, *110*, 2221-2238.
136. Li, Z.; Chen, J.; Shen, J.; Liu, K. Elastic Deformation of Surface Topography under Line Contact and Sliding-rolling Conditions. *Journal of Mechanical Engineering* **2018**, *54*, 142-148.
137. Zhao, J.; Li, Z.; Zhang, H.; Zhu, R. Effect of micro-textures on lubrication characteristics of spur gears under 3D line-contact EHL model. *Industrial Lubrication and Tribology* **2021**, *73*, 1132-1145.
138. Petare, A. C.; Mishra, A.; Palani, I. A.; Jain, N. K. Study of laser texturing assisted abrasive flow finishing for enhancing surface quality and microgeometry of spur gears. *The International Journal of Advanced Manufacturing Technology* **2018**, *101*, 785-799.
139. Pei, X.; Pu, W.; Zhang, Y.; Huang, L. Surface topography and friction coefficient evolution during sliding wear in a mixed lubricated rolling-sliding contact. *Tribology International* **2019**, *137*, 303-312.
140. Morales-Espejel, G. E.; Rycerz, P.; Kadiric, A. Prediction of micropitting damage in gear teeth contacts considering the concurrent effects of surface fatigue and mild wear. *Wear* **2018**, *398-399*, 99-115.
141. Wang, J.; Yan, Z.; Fang, X.; Shen, Z.; Pan, X. Observation and experimental investigation on cavitation effect of friction pair surface texture. *Lubrication Science* **2020**, *32*, 404-414.
142. Xiao, H.; Zhang, F.; Li, Z.; Tang, Y.; Li, L. Gear tribological and contact fatigue prediction with rough topography and groove texture under elastohydrodynamic lubrication. *Meccanica* **2025**, *60*, 2641-2669.
143. Liu, L.; Yang, C.; Sheng, Y. Y. Wear model based on real-time surface roughness and its effect on lubrication regimes. *Tribology International* **2018**, *126*, 16-20.
144. Cheng, G.; Ma, J.; Li, J.; Sun, K.; Wang, K.; Wang, Y. Study on the dynamic characteristics of gears considering surface topography in a mixed lubrication state. *Lubricants* **2023**, *12*, 7.
145. Ruan, J.; Wang, X.; Wang, Y.; Chen, L. Study on anti-scuffing load-bearing thermoelastic lubricating properties of meshing gears with contact interface micro-texture morphology. *Journal of Tribology* **2022**, *144*, 101202.